

Space charge effects in photoemission with a low repetition, high intensity femtosecond laser source

S. Passlack, S. Mathias, O. Andreyev, D. Mitnacht, M. Aeschlimann, and M. Bauer^{a)}

Department of Physics, University of Kaiserslautern, 67663 Kaiserslautern, Germany

(Received 9 September 2005; accepted 29 May 2006; published online 25 July 2006)

In this paper, we present experimental results on the effect of space charging in photoelectron spectroscopy from a surface using a pulsed and intense femtosecond light source. We particularly focus on a quantitative evaluation of the induced spectral broadening. Our results are compared with analytic calculations based on energy conservation considerations as well as with experimental results from measurements using picosecond pulses for the excitation process. As a measure of space charge effects, we monitored the angular and energy distributions of the photoemission from the occupied Shockley surface state of Cu(111) as a function of the total number N of the photoemitted electrons per laser pulse. Our results show that spectral distortions exist for the entire laser fluence regime probed. The energetic broadening of the surface state peak can be fitted with remarkable accuracy by a \sqrt{N} dependence, in agreement with the theoretical predictions and different from the experimental picosecond results, where a dominating linear dependence has been reported. In addition to a pure energetic broadening of the photoemission spectra, we also identify modifications in the angular distribution of the photoemitted electrons due to space charge effects.

© 2006 American Institute of Physics. [DOI: [10.1063/1.2217985](https://doi.org/10.1063/1.2217985)]

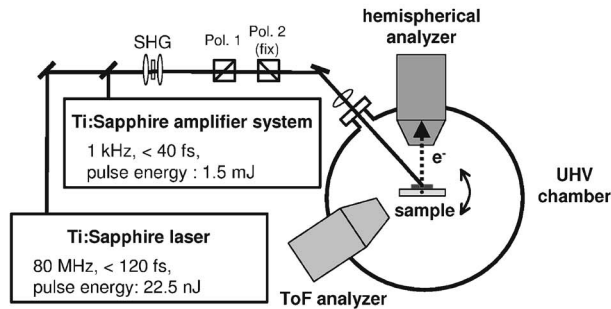
I. INTRODUCTION

The extensive interest in time-resolved photoemission experiments on subpicosecond time scales that has emerged over the last decade has been stimulated by the potential of this technique to provide detailed insights into the real-time dynamics of electronic excitations associated with, for example, the initiating steps in chemical surface reactions.¹ In a two photon photoemission (2PPE) experiment, these excitations can easily be studied using the optical output of a high repetition, pulsed femtosecond laser source. The recent progress in the creation of intense, ultrashort light bunches in the extended ultraviolet (EUV) and x-ray ultraviolet (XUV) regimes by means of high order harmonic generation (HHG) or by the availability of XUV-free electron laser (FEL) sources opens up the potential to extend the accessible binding energy regime into the valence and core level regions for these experiments.^{2–4} This enables further extension of our knowledge on the electronic and nuclear dynamics associated with ultrafast changes in the chemical or magnetic state of a surface. The rather low repetition rate of these sources, which is intrinsic to the creation process of the pulsed XUV radiation, requires high pulse fluences for a time-resolved photoemission experiment to achieve reasonable integration times. As a consequence, the photoemitted electrons will leave the surface in short pulses with a fairly high electron density. Space charge effects due to the Coulomb repulsion between the electrons within such a pulse distort the spectral distribution of these electrons and result in a considerable loss in both energy resolution and angular resolution for the photoemission experiment as has been reported in various publications on picosecond photoemission in the past.^{5–10} In-

dications for space charge effects are, for example, the broadening and shift of the entire spectrum,^{5,6} the appearance of “ghost” peaks in the spectrum,⁶ or the observation of extremely high electron kinetic energies exceeding the used photon energies by several orders of magnitude.^{7,8} Even though these experimental observations have been supported with quite some success by corresponding calculations in these publications (see particularly in Ref. 9), the relevance of space charge effects for high resolution photoelectron spectroscopy has not been addressed until very recently.¹⁰ In their work the authors identify spectral shifts and spectral broadening effects of the Fermi edge of a gold sample of the order of a few meV in a high resolution photoemission experiment using 60 ps synchrotron EUV light pulses. Numerical simulations enable to assign these spectral distortions to space charge effects in the photoemitted electron cloud and to the interaction of the electron cloud with the image charge in the substrate.

From a rather different point of view space charging in photoemission has attracted considerable interest regarding the creation of ultrashort electron bunches, e.g., for the realization of pulsed electron guns for time-resolved electron diffraction experiments.¹¹ Here, the photoemission from a metallic surface, induced by a pulsed pico- or femtosecond light source, is used to create these electron bunches which, again, exhibit distortions by the Coulomb interaction of the electrons. Just recently, two publications have addressed the resulting temporal dispersion of (initially) femtosecond electron pulses from a theoretical point of view, which is of relevance for the achievable time resolution in these diffraction experiments.^{12,13} Even though differently motivated these calculations contain obviously the physics relevant for

^{a)}Author to whom correspondence should be addressed; electronic mail: mkbauer@physik.uni-kl.de

(a) **Experimental set-up:**

(b)

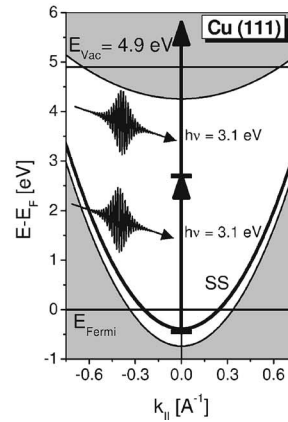


FIG. 1. (a) Scheme of the experimental setup. (b) Projected band structure for the parallel momentum of the Cu(111) surface. The arrows indicate the two photon photoemission-excitation process from the occupied Shockley surface state, which is used to probe the space charge effects induced by intense femtosecond laser pulses.

photoemission and may, therefore, also be used to model, e.g., broadening effects observed in femtosecond photoelectron spectroscopy.

In this paper, we address the question as to which level of electron densities do space charge effects become relevant in a high resolution photoelectron spectroscopy experiment using *femtosecond* light pulses in the *optical* regime. The focus is set on the space charge induced energy broadening. Similar to the experimental approach described in Ref. 10 we used a very defined and narrow feature as a probe for the spectral distortions, in our case the Shockley surface state of a (111)-oriented copper single crystalline surface.

For excitation with a 1 kHz laser system and a kinetic electron energy of about 1 eV, we observe that spectral distortions in the photoemission spectrum in both energy distribution and angular distribution as a result of space charging become apparent even at photoemission yields as low as 1000 *e*/pulse for a source diameter of about 700 μm . Even for these moderate parameters the total energy broadening exceeds the maximum spectral distortions reported in Ref. 10 for excitation with a 60 ps EUV pulse by a factor of 4. Our experimental data are compared with predictions based on analytical calculations for femtosecond electron pulses presented in Ref. 12. We find a qualitative and quantitative very good agreement confirming a \sqrt{N} dependence of the energy broadening for photoemission initiated by femtosecond laser pulses, where N is the number of electrons in the electron pulse. Note that for excitation with picosecond light sources a dominating linear dependence of the broadening has been reported before.^{5,10}

II. EXPERIMENTAL SETUP

The principle scheme of the monochromatic time-resolved 2PPE setup used for these studies is shown in Fig. 1(a). The high intensity laser source is a commercial 1 kHz multipass femtosecond Ti:sapphire amplifier system (Quantronics, "Odin") pumped by the second harmonic of a *Q*-switched Nd:YLF laser (Quantronics Model 527) and seeded by a sub-20-fs Ti:sapphire oscillator (KML-MTS kit). At an average power of 1.5 W, the amplifier provides sub-40-fs laser pulses with a central wavelength at 800 nm. For the 2PPE experiments, the output of this system is frequency doubled in a 0.7 mm thick beta barium borate (BBO) crystal.

The *p*-polarized light then passes through a lens ($f = 1000$ mm) and hits the sample at an angle of 45° . Due to this projection, the laser spot on the sample surface is elliptical with a long axis of 1.15 mm [full width at half maximum (FWHM)] and a short axis of 0.9 mm (FWHM), as measured *ex situ* by beam profile analysis at a corresponding distance from the lens. The power of the incident laser pulses and, therefore, the photoemission yield can be adjusted by a pair of polarizers.

For reference, two photon photoemission spectra were also recorded using the *p*-polarized frequency doubled output of a narrow band, pulsed Ti:sapphire oscillator (Spectra-Physics, Tsunami, 80 MHz, 125 fs, 1.8 W average power). In this case, the laser light was focused onto the sample using a 250 mm lens resulting in a beam diameter of about 150 μm at the surface.

For detection of the photoemitted electrons, the UHV chamber is equipped with two different types of energy analyzers. The first system is a 150 mm hemispherical electron energy analyzer (SPECS Phoibos 150) including a two-dimensional (2D)-detection unit, which consists of a micro-channel plate (MCP), a phosphorus screen, and a charge-coupled device (CCD) camera. This configuration allows a parallel and, therefore, highly efficient mapping of the energy distribution and angular distribution, $E(\varphi)$, of the photoemission signal. At a pass energy of 20 eV, a kinetic energy range of 2.5 eV, and an angular spread of 12° are covered simultaneously. The energy resolution of the analyzer in the present study was <20 meV at an angular resolution of less than 0.15° .

The second system consists of a home-built electron time-of-flight analyzer with a 300 mm drift tube and a 28 mm diameter detector corresponding to an acceptance angle of 3° . The $50\ \Omega$ impedance matched anode of the detection unit allows for signal acquisition almost free of ringing so that efficient multihit detection per laser shot is possible. This enables distortion-free recording of 2PPE spectra up to an average count rate of 4 *e*/laser pulse. For experiments performed with the time-of-flight (TOF) detector, an extraction bias of 1.5 V was applied to the sample. In general, the rather high efficiency (no energy-scanning neces-

sary) of both electron energy analyzers makes these systems highly preferable for photoemission experiments performed with low repetition light sources.

To accurately measure the total 2PPE current from the sample surface, which is required to determine the average number of electrons emitted by a single laser pulse, the total photoemission current has been measured using a commercial picoamperemeter (Keithley model 485).

The Cu(111) crystal was cleaned by repeated sputtering (10 min, 500 V) and annealing cycles (15 min, 500 °C). Prior to measurement, the surface quality was checked by low energy electron diffraction (LEED), Auger spectroscopy, and the photoemission characteristics of the Shockley surface state of the Cu(111) surface.

III. EXPERIMENTAL RESULTS AND DISCUSSION

To quantify the effects of space charging, we performed 2PPE on the occupied Shockley surface state of a Cu(111) surface. The existence of this particular state has been proposed by Shockley¹⁴ as the result of the termination of bulk material by its surface. Experimentally, this state was confirmed by Gartland and Slagsvold.¹⁵ For Cu(111) at 300 K, the Shockley surface state is located in the L_2' - L_1 gap of the Cu(111) crystal at a binding energy of 390 meV [see Fig. 1(b)].¹⁶ As a model system to study many-body effects such as electron-electron and electron-phonon interactions, the spectral characteristics of these states have been the focus of numerous photoemission and scanning tunneling microscopy experiments in the past (see Ref. 17 and references therein). A 2PPE map of the Cu(111) crystal recorded with the 2D-hemispherical analyzer using the second harmonic (3.1 eV) of the high repetition laser system (oscillator) is shown in Fig. 2(a). Clearly visible as a white line is the photoemission from the surface state exhibiting its characteristic dispersion with emission angle φ . The laser pulse fluence incident onto the sample surface is 11×10^{-3} mJ/cm² (spot diameter at the surface: 150 μ m). The integral photoemission yield is about 3 *e*/pulse. For the Shockley surface state, we measure with these experimental conditions a linewidth of 86 meV. This value contains the homogeneous linewidth of the surface state as well as inhomogeneous contributions, such as spectrometer resolution (20 meV), laser bandwidth (25 meV), and broadening effects due to imperfections of the surface. We exclude, however, significant contributions due to space charge broadening at these low electron yields (per pulse). This assumption is supported by our calculations based on an analytical model as described in Ref. 12 and introduced later in this paper. At these conditions, the model predicts a space charge broadening of <3 meV. The measured angular dispersion in this reference experiment corresponds to an effective mass of the Shockley surface state of $m^*/m=0.42(2)$. The measured binding energy, linewidth, and effective mass are in good agreement with reference literature values at room temperature.¹⁶ In the following discussion, the linewidth value of 86 meV will be referred to as the “intrinsic” linewidth of the surface state and will be used as a reference for the subsequent experiments using the high intensity, low repetition laser system.

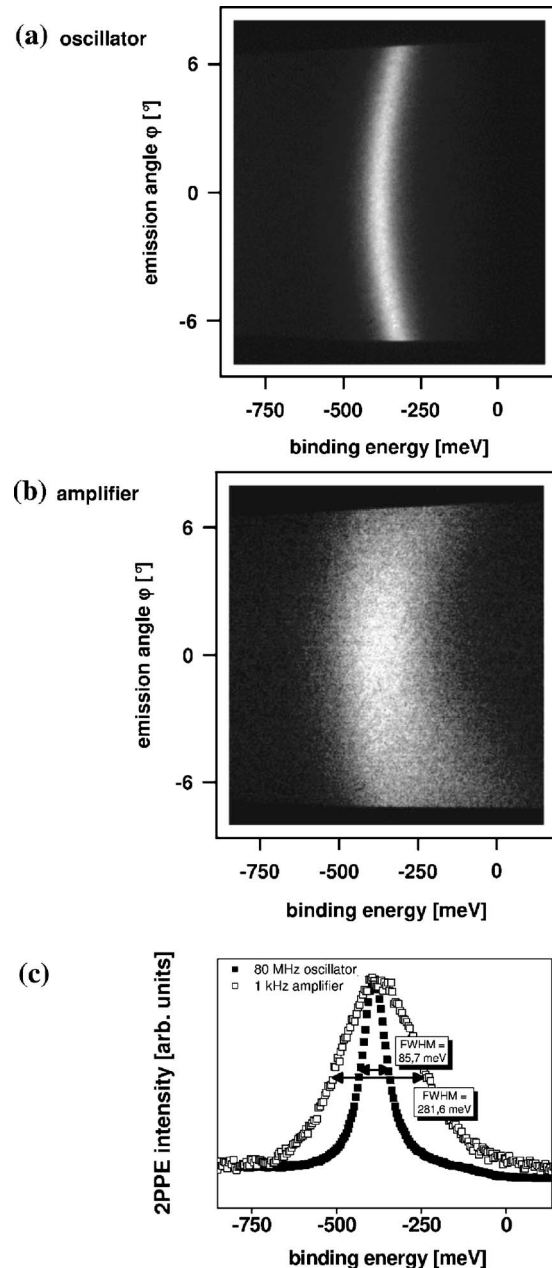


FIG. 2. (a) 2PPE $E(\varphi)$ map of the Cu(111) surface recorded using the second harmonic of the 80 MHz laser system. The main signal is due to the dispersing Shockley surface state. (b) Equivalent 2PPE map recorded with the second harmonic of the 1 kHz laser system. A total of about 80 000 *e*/incident laser pulse is emitted from the surface in this experiment. (c) Comparing the 2PPE spectra for normal emission taken from (a) and (b) highlights the strong distortions of the spectral distribution due to space charging.

2PPE experiments using the second harmonic of the 1 kHz amplifier system have been performed under almost identical conditions. However, the spot diameter at the surface had to be expanded for these experiments to about 1 mm to avoid damage of the sample at the highest intensity levels used. Figure 2(b) shows a 2PPE map recorded at an incident pulse fluence of 0.65 mJ/cm². Clearly visible is a drastic distortion of the spectral distribution in comparison to Fig. 2(a). The integral photoemission yield in this experiment was about 80 000 *e*/pulse. After taking into account the increase in the source diameter, this number corresponds to an

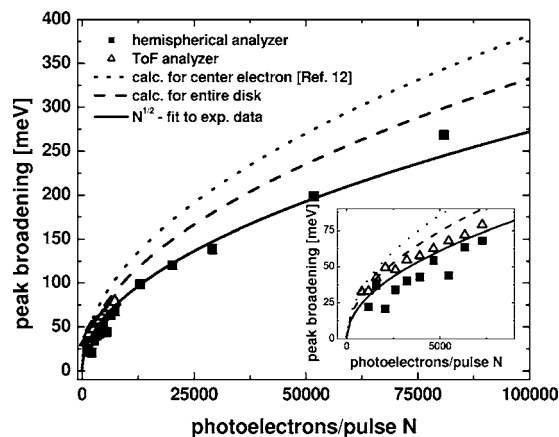


FIG. 3. Kinetic energy broadening ΔE_k of the Shockley surface state as a function of the total number N of photoelectrons emitted per pulse. Solid squares are experimental results obtained using the hemispherical analyzer and the open triangles are TOF data. The solid line is an $N^{1/2}$ dependence fit to the experimental data as predicted by Eq. (4). The dotted line results from a calculation of the space charge broadening for an electron in the center of the charge cloud following Siwick *et al.* (Ref. 12); dashed line: same model, but also taking into account the fact that electrons from the entire charge cloud are detected by the energy analyzer. The inset highlights the dependence of the line broadening at low photoemission yields.

increase in the charge density of the emitted electron pulse by a factor of about 600 in comparison to the experiment using the high repetition laser system.

Figure 2(c) directly compares the 2PPE spectra at normal emission extracted from Figs. 2(a) and 2(b). The spectral distortions due to the coulomb interaction between the electrons emitted for excitation with the intense 1 kHz laser and the 80 MHz laser system are rather striking. A significant broadening of the surface state accompanied by a clear development of an asymmetric line shape of the surface state peak is observed. Furthermore, the center of gravity of the surface state shifts to a lower binding energy. In addition, these space charge induced changes are not restricted to the surface state. In general and in agreement with other publications^{5,6,9,10} all features in the spectrum (e.g., low energetic onset and Fermi edge) undergo an energetic broadening and the entire width of the 2PPE spectrum increases with the number of photoemitted electrons.

The narrow Shockley surface state with its well defined dispersion makes it an ideal probe to monitor and quantify the space charge effect on photoemitted electrons in more detail. Next, we will focus on the spectral modifications of the Shockley surface state as a function of the total number of the electrons N photoemitted per incident laser pulse. The energy broadening ΔE_k of the surface state peak is plotted as a function of N in Fig. 3. ΔE_k was determined by quadratic subtraction of the intrinsic linewidth (86 meV) from the linewidth of the Shockley surface state as measured in the 1kHz-2PPE experiments. The solid squares in Fig. 3 correspond to the broadening of the surface state as measured using the hemispherical 2D electron energy analyzer system. For the entire intensity regime, we observe clear modifications of the detected spectral distribution from the surface state due to space charging. The width of the surface state peak increases monotonically with increasing photoelectron yield. For N

$> 10\,000$ the space charge induced broadening becomes even larger than the intrinsic linewidth of the Shockley surface state. For the highest laser intensities used in this experiment the broadening exceeds this value by more than a factor 3. We conclude that for a meaningful spectroscopy of the Shockley surface state under the present experimental conditions integral photoemission yields has to be kept below a value of about 3000 e /pulse. Only this requirement guarantees that the space charge induced broadening is significantly smaller than the intrinsic linewidth of the surface state.

Intuitively, space charge broadening is most efficient when the photoemitted electron pulse exhibits a large charge density. This is obviously the case right after the emission in front of the copper surface, but before significant dispersion of the propagating electron pulse has occurred. Furthermore, the entrance lens system of the used hemispherical analyzer exhibits a single focus so that the initial electron pulse will be recombined again. Therefore, this point may act as an additional source of space charge broadening. Indeed, in case of other electron detection schemes such as photoemission electron microscopy, relevant space charging in the analyzing device has been noted before.¹⁸ To check the influence of the entrance lens system on the measured spectral distribution, we performed identical photoemission experiments with the 1 kHz amplifier system using an electron TOF analyzer. Except for an acceleration of the photoemitted electrons towards the entrance of the TOF drift tube due to the applied bias voltage of 1.5 V, the electrons can, in this detection scheme, propagate and disperse freely within the analyzer unit. Therefore, only space charge effects intrinsic to the photoemission process at the sample surface are monitored. Experiments using the TOF analyzer could be performed up to $N=7500$ e /pulse resulting in a detected count rate of up to 4 e /pulse in the TOF detector. For higher currents, overexposure of the MCP detector resulted in noticeable distortions of the measured spectral distribution. Analogous to the measurements using the hemispherical analyzer, data analysis was performed by quadratic subtraction of the intrinsic linewidth from the measured linewidth of the Shockley surface state. The obtained TOF data are included as open triangles in the inset of Fig. 3. For the probed electron density region, we find a very good agreement between both experimental data sets. We attribute the very small, but systematic, shift of the TOF data towards larger values to the slightly higher kinetic energy (and, consequently, higher group velocity) in the relevant space charge region due to the applied bias voltage in the TOF experiment [see Eq. (1) below]. Despite this shift, we conclude that space charge effects within the lens system of the used hemispherical analyzer are not relevant, at least below the electron density regime accessible within the TOF measurements.

The magnitude of space charge broadening as function of the number of emitted electrons per laser pulse can be estimated based on an analytical expression following the work by Siwick *et al.* on the propagation dynamics of femtosecond electron packets.¹² Equation (5) in this reference approximates the space charge induced kinetic energy bandwidth ΔE_k for a disk of electrons as function of propagation time t to

$$\Delta E_k(t) \approx mv_0 \Delta v = mv_0 \frac{dl}{dt}, \quad (1)$$

where m is the electron mass, v_0 is the group velocity (center of mass velocity) of the emitted electron pulse, and dl/dt is the rate of lateral broadening of the electron bunch into the direction of pulse propagation. The dominant contribution to space charge broadening happens within the first 10 ns after emission.¹² Taking into account the average (group) velocity of the electron pulse of 2.5×10^5 m/s the propagation distance for the present experiment is about 2.5 mm on this time scale. Energy analysis of the photoemitted electron pulse is performed at much larger distances, hence the limiting case of $t \rightarrow \infty$ should be sufficient to describe the present experimental configuration. Due to energy conservation the entire initial Coulomb energy of the emitted electron cloud will be transformed into the total kinetic energy bandwidth ΔE_k so that $\Delta v = dl/dt$ can be directly related to the potential energy V of the electron pulse at $t=0$ by¹⁹

$$\frac{dl}{dt} = \left(\frac{2V}{m} \right)^{1/2}. \quad (2)$$

For example, for electrons located right in the center of the propagating charge disk the potential energy V is given by

$$V = \frac{eN}{2\epsilon_0\pi r_0}, \quad (3)$$

where e is the electron charge, ϵ_0 is the permittivity of free space, r_0 is the radius of the electron beam, and N is the number of electrons in the pulse.

According to Eq. (2) the velocity spread $\Delta v = dl/dt$ finally added to these electrons is, therefore, given by

$$\Delta v = \frac{dl}{dt} = \sqrt{\frac{2V(z=0)}{m}} = \left(\frac{e}{m\epsilon_0\pi r_0} \right)^{1/2} N^{1/2}. \quad (4)$$

The first important point to note in comparison to the experimental data is that the predicted $N^{1/2}$ dependence of the space charge broadening is almost perfectly reproduced. A corresponding fit to our data is shown as solid line in Fig. 3.

Using realistic electron cloud parameters, the experimental data can also be quantitatively reproduced by this model reasonably well. The extension of the electron pulse perpendicular to its propagation direction can be approximated by a disk with a radius $r_0 = 0.35$ mm, which is estimated from the cross section of the incident light pulse and takes into consideration the second order nonlinearity of the 2PPE process. As the area of a Gaussian emission profile defined by a FWHM corresponding to this radius contains only about half of the totally emitted electrons N the effective number of electrons for a calculation that corresponds to our experiment must be reduced to $N/2$. We then estimate the group velocity of the emitted electron pulse from the weighted average of the spectral 2PPE electron distribution to be 2.5×10^5 m/s, which corresponds to an average kinetic energy of 0.18 eV.²⁰ The broadening ΔE_k expected from

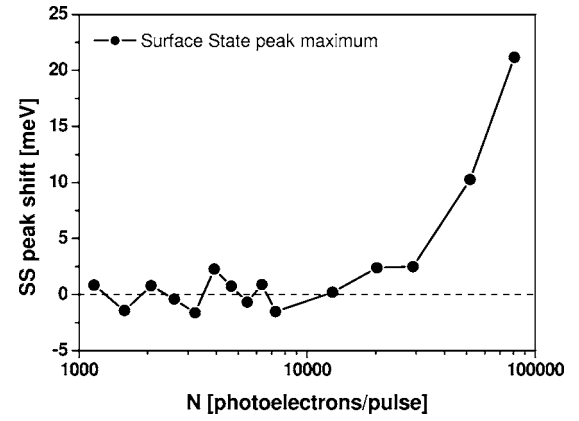


FIG. 4. Energy shift of the Shockley surface state peak maximum as function of the total number of photoemitted electrons per laser pulse. Particularly for the highest electron yields, we observe a shift to lower binding energies that we attribute to momentum blurring induced by space charging. The shift to lower binding energies is accompanied by the evolution of an asymmetric line shape of the surface state peak [see Fig. 2(c)].

Eqs. (1) and (4) for an electron located in the center of the photoemitted cloud under these conditions is displayed in Fig. 3 as a dotted line.

However, in the photoemission experiment, the detected electrons originate not only from the center of the charge cloud but also from the rest of its volume. Therefore, a more accurate quantification of the expected space charge broadening requires a correction to Eq. (4) to account for the potential energy variations along the radius of the electron cloud. In general, this dependence cannot be given in a closed analytical expression. A linear approximation can be derived, however, using the available analytical expressions for the center potential [Eq. (3)] and the potential at the border of a disk given by $V = (eN)/(\pi\epsilon_0\pi r_0)$. Equation (4) then becomes

$$\Delta v = \left[\frac{e}{m\epsilon_0\pi r_0} \left(\frac{2}{3\pi} + \frac{1}{6} \right) \right]^{1/2} N^{1/2}. \quad (5)$$

The result of the calculation for ΔE_k using Eq. (5) is shown as a dashed line in Fig. 3 where the calculation produces a rather good estimate of the space charge broadening. Our experimental values are overestimated only by a factor of about 1.2. We assume that the residual deviation between experiment and theory is due to assumptions regarding the radial dependence of the initial potential energy. Additionally, we have not explicitly considered that the electron density is also a function of radius where the dependence follows the intensity profile of the exciting laser pulse.

In addition to broadening the linewidth, the increase in emission density results in two additional modifications to the Shockley surface state spectrum. First, an energetic shift of the peak maximum to lower binding energies is observed (see Fig. 4), starting at $N > 40,000$. Second, the shape of the Shockley surface state evolves to show a clear asymmetry with increasing laser fluence [see Fig. 2(c)]. Peak shift and asymmetric line shapes in the photoemission from the Shockley surface state are well-known effects associated with limitations in the angular resolution of the experimental setup²¹ or with structural inhomogeneities (imperfections) of

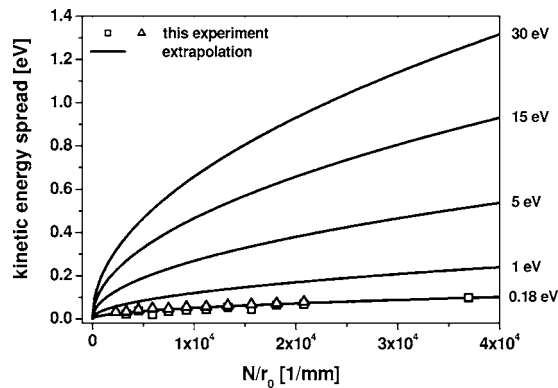


FIG. 5. Extrapolation of the $N^{1/2}$ dependence deduced from our experimental data to photoemission experiments performed at higher kinetic electron energies where r_0 is the radius of the emitted electron cloud. The energy labeling at the right of the graph is related to the group velocity of the photoemitted electron cloud.

the investigated surface.²² Due to partial loss of angular information regarding the surface state dispersion in both cases, electrons with finite k_{\parallel} are detected in the “normal emission” experimental configuration. The upwards dispersion of the Shockley surface state causes these electrons to always contribute to the photoemission signal at lower binding energies than the binding energy maximum of the surface state at the Γ point. Such momentum blurring must result in the characteristic shape asymmetry and the peak shifting towards the Fermi edge, which are experimentally observed here. In this context, we assign the spectral changes identified in our study to loss of angular information induced by a modification of the electron trajectories due to Coulomb interactions within the charge cloud.

Let us compare our femtosecond results with high resolution photoemission data under picosecond synchrotron excitation available from Ref. 10. We identify two general differences between both experiments. Firstly, the extension of the nascent electron bunch along the propagation direction right after excitation differs by a factor of about 10^3 (40 fs versus 60 ps), as it is determined by the temporal width of the exciting light source. Secondly, the initial kinetic energy distribution in our experiment is 1.2 eV in comparison to 30 eV in the synchrotron experiment. Note that the spatial extension of the two electron beams perpendicular to the propagation direction (transversal extension) is rather comparable as given by a beam radius of $r_0 \approx 0.35$ mm in our experiment and a rectangular beam profile of about 0.45×0.45 mm² for the synchrotron excitation. For the experimental results we find that the magnitude of broadening is much larger in the femtosecond case than in the picosecond case. For example, for $N=1250$, our femtosecond experiment values exceed the Fermi-level broadening in Ref. 10 by a factor of 4. Even more, if we take into account the difference in the electron kinetic energy in both experiments (0.7 eV versus 30 eV), which is also relevant for the magnitude of the energy broadening [see Eq. (1)], this factor increases up to a value of about 10 (see also discussion below and Fig. 5). This difference can directly be assigned to the difference in the Coulomb energy V initially stored by the respective na-

scient electron pulses for a given number N of electrons. Due to its much smaller extension the value of V must be increased for the femtosecond pulse.

The Monte Carlo simulations in Ref. 10 accompanying the experimental studies using picosecond excitation showed that the Coulomb interaction between the electrons alone was not sufficient to describe quantitatively the observed spectral modifications regarding energy broadening and energy shift. Instead, also the interaction of the electron cloud with its own mirror charge induced inside the metallic substrate had to be considered to achieve a satisfactory agreement between experiment and calculation. The analytic expressions used in our work exclusively consider electron-electron Coulomb interaction within the electron pulse. The observed good agreement between our experimental data and this quantitative description gives strong indication that mirror charge effects are of less relevance for electron pulses created by femtosecond excitation. In addition, the interaction of an electron pulse with its mirror charge gives rise to retardation effects so that for sufficient high excitation densities even a recapture of low energy electrons by the surface should be noticeable. We do not observe any significant reduction of the photoemission yield in the low energy tail of the spectrum even at the highest emission currents, which we take as an additional evidence that mirror charge interaction is of minor relevance in our experiment. We interpret this difference between picosecond and femtosecond experiments as follows. The mirror charge potential induced by the electron pulse is mainly governed by the total number N of electrons within the electron cloud and is, therefore, in first order independent on the lateral extension of the electron pulse. In contrast, the Coulomb energy V increases with increasing charge density and, therefore, decreasing lateral extension of the electron pulse. The picosecond pulse properties are obviously equally governed by Coulomb interaction *and* mirror charge effects. In contrast, in the case of the femtosecond excitation the Coulomb energy V dominates the energy broadening effect due to the much smaller lateral extension of the electron pulse so that mirror charge distortions of the spectral distribution stay hidden.

The differences in the respective pulse parameters also affect the detailed dependence of the energy broadening on the number N of electrons within the pulse. In contrast to our \sqrt{N} result, Zhou *et al.* report a linear dependence of the energy broadening on N for $N \geq 500$ (note, however, a possible reminiscent to a \sqrt{N} behavior for rather low sample currents noticeable in Fig. 5 of Ref. 10. This linear dependence for picosecond excitation is also supported by results presented in Ref. 4, deduced from the spectral broadening of an entire photoemission spectrum. Again, the difference in the longitudinal extension of the pulses may be a possible origin of this deviation. For the picosecond electron pulse the longitudinal extension (0.2 mm) is of the order of the transversal extension (0.42 mm). Therefore and in contrast to the femtosecond pulse, the electron bunch cannot be approximated by a disk. The closed analytic form for the potential energy within the electron cloud given by Eq. (3) is not applicable to estimate the space charge broadening for the picosecond case. Instead, numerical calculations have to be used, which

can reproduce the dominating linear dependence of the energy broadening for picosecond excitation rather well.^{4,10} The deviation from the disk case entails another consequence. Whereas the magnitude of the space charge broadening in the femtosecond case is determined only by N/r_0 as given by Eq. (4), for picosecond pulses the longitudinal extension should also become relevant. Thus, in a typical picosecond photoemission experiment, the space charge broadening is sensitive to the pulsewidth of the exciting light source in agreement with the numerical calculations in Ref. 10.

Finally, we would like to compare the results regarding the energy shift of a spectral feature in both experiments. Again, we identify a striking difference between the femtosecond and the picosecond experiments. In the latter case, a clear linear dependence of the energy shift towards higher kinetic energies has been reported, which extends down to the lowest electron densities probed (of the order of 100 *e*/pulse). The magnitude of the shift is of the same order as the energy broadening. This is in striking contrast to our results, where we observe no indications for any shift up to a level of at least 10 000 *e*/pulse (see Fig. 4) even though the energy broadening has already reached a value of 90 meV (see Fig. 3). Again, for the picosecond case the numerical calculations could show that the energy shift is governed by space charge and image charge effects. We cannot exclude that the energy shift observed for the very high electron density regime may arise partly from the space charge and image charge effects. The evolvement of the characteristic asymmetry in the line shape points, however, to a dominant contribution to this shift by momentum blurring as discussed above.

Based on the exceptionally good agreement between the predicted $N^{1/2}$ dependence of energy broadening and our experimental results, we can extrapolate our experimental data to higher photoelectron energies up to several tens of an eV. This energy regime is relevant for time-resolved photoemission experiments using high-order harmonic sources or most recent FEL facilities. Equation (1) gives the relation between energy broadening ΔE_k and the (average) velocity v_0 (and, therefore, kinetic energy) of the emitted electron bunch. As dl/dt is determined only by the Coulomb energy in the initial state and is independent of the group velocity of the electron bunch, extrapolation is performed by scaling our experimental results by v'_0/v_0 , where v_0 and v'_0 are the group velocities of the electron pulse in the present experiment (2.5×10^5 m/s) and the electron pulse under consideration, respectively. The different lines in Fig. 5 show these extrapolations to experiments performed at different mean kinetic energies (group velocities) of the photoemitted electron cloud compared to the present results. Note that the kinetic energy broadening in this graph is displayed now as function of N/r_0 , which is the relevant parameter determining the spectral space charge broadening ΔE_k of a narrow disk of photoemitted electrons [see Eq. (4)— $l/r_0 \ll 1$, where l is the length of the electron pulse in the direction of propagation]. As expected from Eq. (1), the absolute value of energetic space charge broadening ΔE_k becomes larger for higher kinetic energies even though $\Delta E_k/E_{kin}$ is reduced. Therefore,

Fig. 5 allows estimating the maximum allowed number of emitted electrons per pulse to achieve a predefined energy resolution in the experiment.

IV. SUMMARY

We have studied the effect of space charging in a femtosecond two photon photoemission experiment where the kinetic energy is less than 3 eV using an intense, 1 kHz pulsed laser source. Spectral distortions are observed for the entire intensity regime probed. The induced energetic broadening ΔE_k has been quantified by spectroscopy of the Shockley surface state for Cu(111). We show that ΔE_k scales with the square root of the total number of electrons N photoemitted per incident laser pulse, which is in agreement with theoretical predictions for femtosecond excitation by Siwick *et al.*¹² In contrast, for picosecond excitation a rather linear dependence on N has been predicted and observed experimentally before.^{5,10} We show that the qualitative and quantitative differences between the femtosecond and picosecond results are mainly governed by the difference in the longitudinal extension of the electron pulses in relation to their transversal extension. In addition to linewidth broadening, we also observe a modification in the angular distribution of the photoemitted electrons similar to results reported for photoemission from a surface exhibiting a high defect density or for experiments performed using a restricted energy resolution. From the data collected at low kinetic electron energies and an analytical expression derived in Ref. 12, we are able to extrapolate the magnitude of space charge broadening at the higher kinetic electron energies relevant for photoemission experiments at UV excitation. The general trend is an increase in the absolute energy broadening ΔE_k as the mean kinetic energy of the emitted electron cloud increases.

ACKNOWLEDGMENTS

Special thanks go to O. Heinz, B. Siwick, and F. v. Meyer zu Heringdorf for helpful discussions and suggestions. In addition, the authors are grateful to J. Dean for critical comments on various aspects of this manuscript. This work was supported by the Deutsche Forschungsgemeinschaft through SPP 1093 and the Stiftung Innovation Rheinland-Pfalz.

¹H. Petek and S. Ogawa, *Prog. Surf. Sci.* **56**, 239 (1997); M. Bauer, *J. Phys. D* **38**, R253 (2005).

²R. Haight, *Appl. Opt.* **35**, 6445 (1996).

³M. Bauer, C.-F. Lei, K. Read, R. Tobey, J. Gland, M. M. Murnane, and H. C. Kapteyn, *Phys. Rev. Lett.* **87**, 025501 (2001).

⁴P. Siffalovic, M. Drescher, and U. Heinzmann, *Europhys. Lett.* **60**, 924 (2002).

⁵R. Clauser and A. Blacha, *J. Appl. Phys.* **65**, 4095 (1989).

⁶T. L. Gilton, J. P. Cowin, G. D. Kubiak, and A. V. Hamza, *J. Appl. Phys.* **68**, 4802 (1990).

⁷Gy. Farkas and C. Toth, *Phys. Rev. A* **41**, 4123 (1990).

⁸C. Girardeau-Montaut and J. P. Girardeau-Montaut, *Phys. Rev. A* **44**, 1409 (1991).

⁹D. M. Riffe, X. Y. Wang, M. C. Downer, D. L. Fisher, T. Tajima, J. L. Erskine, and R. M. More, *J. Opt. Soc. Am. B* **10**, 1424 (1993).

¹⁰X. J. Zhou *et al.*, *J. Electron Spectrosc. Relat. Phenom.* **142**, 27 (2005).

¹¹E. Hull, J. Cao, C. A. Schmittenmaer, L. G. Jahn, Y. Gao, H. E. Elsayed-Ali, D. A. Mantell, and M. R. Scheinfein, *Rev. Sci. Instrum.* **66**, 1000 (1995).

- ¹²B. J. Siwick, J. R. Dwyer, R. E. Jordan, and R. J. Dwayne Miller, *J. Appl. Phys.* **92**, 1643 (2002).
- ¹³B.-L. Qian and H. E. Elsayed-Ali, *J. Appl. Phys.* **91**, 462 (2002).
- ¹⁴W. Shockley, *Phys. Rev.* **56**, 317 (1939).
- ¹⁵P. O. Gartland and B. J. Slagsvold, *Phys. Rev. B* **12**, 4047 (1975).
- ¹⁶R. Matzdorf, G. Meister, and A. Goldmann, *Phys. Rev. B* **54**, 14807 (1996).
- ¹⁷F. Reinert, G. Nicolay, S. Schmidt, D. Ehm, and S. Hüfner, *Phys. Rev. B* **63**, 115415 (2001).
- ¹⁸F. Meyer zu Heringdorf (private communication).
- ¹⁹B. J. Siwick (private communication).
- ²⁰To account for the energy dependent emission characteristic and transmission probability of the analyzer this weighting was performed using a 2PPE-spectra recorded at an applied extraction bias of 5 eV, significantly larger than the width of the spectral distribution of 1.2 eV.
- ²¹R. Panagio, R. Matzdorf, G. Meister, and A. Goldmann, *Surf. Sci.* **336**, 113 (1995).
- ²²A. Beckmann, K. Meinel, Ch. Ammer, M. Heiler, and H. Neddermeyer, *Surf. Sci. Lett.* **375**, L363 (1997).